Optimized IIR Filter Applied to the Limiting and Filtering Technique for Peak-to-Average Power Ratio Reduction

Felipe Artemio Schoulten and Eduardo Gonçalves de Lima
Grupo de Circuitos Integrados e Sistemas (GICS) – Departamento de Engenharia Elétrica
Universidade Federal do Paraná, Curitiba, Brazil

***Abstract*—To improve the efficiency of wireless transmitters, the peak-to-average power ratio (PAPR) of complex-valued envelope signals can be reduced through a limiting and filtering technique. A constrained nonlinear optimization tool is reported in literature for the identification of the clipping factor and a finite impulse response (FIR) filter. In this work, such tool is extended to handle the identification of an infinite impulse response (IIR) filter. The extension is not straightforward because IIR filters can exhibit instability and the nonlinear optimizer becomes more susceptible to be trapped into local minima. An additional constraint is incorporated here to guarantee stability and coefficients from a Butterworth low-pass filter are chosen as an initial guess for the identification procedure. Matlab simulation results from a case study that employs a WCDMA envelope signal show that an extra PAPR reduction of 1.5 dB is achieved by adopting the optimized IIR filter instead of an optimized FIR filter, where this number is equivalent to 15.5% of the initial PAPR value.**

Keywords—Constrained nonlinear optimization, finite impulse response filter, infinite impulse response filter, power amplifier, radio frequency, wireless communication systems.

I. INTRODUCTION

The power amplifier (PA) is the device that consumes the highest amount of power in a wireless communication system [1]. Increasing its efficiency is extremely beneficial for extending the battery autonomy in handsets and reducing the costs in base stations. PA efficiency improves with the increase of average output power [2]. To explore its most efficient behavior, the PA is put to operate at regimes of strong power gain compression, near saturation [2]. Then, the generated nonlinearities are compensated through a digital baseband predistorter (DPD) having an inverse characteristic with respect to the PA [3]. In an ideal scenario, the cascade connection of DPD followed by PA exhibits a linear relationship up to the saturation point. Besides, at a fixed peak level, any reduction in the peak-to-average power ratio (PAPR) of the envelope signal is translated into an increase in average power. Considering that some amount of distortions inside and outside the signal main channel is accepted, any available distortion margin can be exploited to further improve the efficiency [4]. An example of such crest factor reduction (CFR) technique is the limiting and filtering approach [5]. The limiter clips the signal peaks and the filter attenuates the distortions at adjacent channels. In [6], a constrained nonlinear optimization is presented to identify, at the same time and based on the overall system behavior, the limiter clipping factor as well as the taps of a finite impulse response (FIR) filter. However, such approach cannot be directly applied to the identification of a limiter followed by an infinite impulse response (IIR) filter, due to instability issues. Moreover, the nonlinear training tends to become more susceptible to be trapped into local minima in presence of the IIR filter, compared to the FIR filter case. The contribution of this work is to expand the constrained optimizer by including an additional restriction to avoid instability problems and to illustrate an example of good initial guess for the IIR filter poles and zeros, based on the Butterworth low-pass filter [7].

This work is organized as follows. Section II details the limiting and filtering technique. Section III describes the FIR and IIR digital filters. Section IV addresses the CFR parameter identification based on a constrained nonlinear optimization. Section V reports Matlab results from a case study. Conclusions are given in Section VI.

II. LIMITING AND FILTERING TECHNIQUE FOR PAPR REDUCTION

The CFR technique has the purpose to reduce the PAPR of complex-valued envelope signals. A very popular CFR technique consists of a set of two cascaded blocks represented by a limiter followed by a linear digital filter, as shown in Fig. 1.

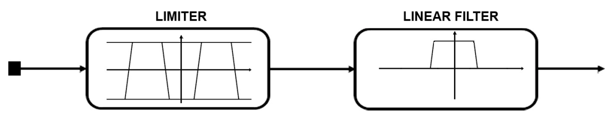

Fig. 1. Block diagram of limiting and filtering technique.

The CFR first block is the hard-clipping limiter [8]. This limiter class clips signal peaks whose amplitudes surpass a pre-defined value, whereas time domain samples having amplitudes below the threshold are kept unchanged. It should be noticed that, for complex-valued envelope signals, a hard-clipping limiter only changes the signal amplitude, thus the signal phase remains unchanged. The hard-clipping limiter mathematical representation, in time domain, is given by:

$$x[n] = \begin{cases} w[n] & ,|w[n]| < L \\ L\exp\{j\angle w[n]\} & ,|w[n]| \geq L \end{cases} \qquad (1)$$

where $w[n]$ is the input signal and $x[n]$ the output signal. The hard-clipping limiter has only one real-valued parameter, namely the clipping factor L, whose value is chosen, in this work, based on an optimization tool.

The purpose of the CFR limiter is to reduce the PAPR by clipping the signal peaks. However, such task can only be performed at the expense of generating significant distortion levels inside and outside the signal main channel.

III. Linear Digital Filters

Linear digital filters represent the CFR second block. Their goal is to partially correct the distortions caused by the limiter block at adjacent channels. This filter block restores to some extent the signal peaks clipped by the CFR first block, therefore causing an increase in PAPR value. Notice that there is an exchange between PAPR value and signal distortions.

In this work, two types of linear digital filters are addressed: finite impulse response (FIR) and infinite impulse response (IIR).

A. FIR Filter

The FIR filter is a linear digital class where the output signal in a certain instant of time depends of the input signals at current and past times and of filter coefficients [9-10]. The FIR filter mathematical representation is given by:

$$y[n] = \sum_{k=0}^{M-1} h_k x[n-k] \qquad (2)$$

where h_k are FIR filter coefficients, M the FIR filter order, $y[n]$ and $x[n]$ the FIR filter output and input complex-valued signals, respectively. The number of FIR filter coefficients, or equivalently the number of past input samples that influences the present output plus one, is given by the filter order. It is noted that the FIR filter does not have any feedback and, hence, it is immune to instability problems.

B. IIR Filter

More general than the FIR filter, the IIR filter is a class of linear digital filters whose output signal in a certain instant of time depends of the input signals in current and past times, like FIR filter, and of the sampled output signals in past times. Thus, in opposite of the FIR filter, the IIR filter has negative feedback, what could foment the instability problem [9-10]. In discrete time, the instability problem arises when there is at least one pole whose amplitude is greater than or equal to the unitary value.

Starting from the constant coefficient linear difference equation and after some algebraic manipulations, the mathematical representation of the IIR filter is obtained as [11]:

$$y[n] = \frac{\sum_{m=0}^{M-1} b_m x[n-m] - \sum_{k=1}^{N-1} a_k y[n-k]}{a_0} \qquad (3)$$

where b_m are the filter coefficients associated to input signals, a_k the filter coefficients associated to output signals in past times, a_0 the coefficient associated to output signal in current time, M and N the numbers of filter coefficients associated to input and output signals respectively, where these numbers subtracted by 1 are the number of considered past samples. The FIR filter can be seen as a particular instance of the IIR filter, obtained when N is set to 0 and a_0 to 1 in (3).

IV. CFR Parameter Identification

In this work, the limiter clipping factor L from (1), as well as the filter coefficients, either h_k from (2) or a_0, a_k and b_m from (3), are chosen based on the following constrained optimization. The optimization goal is to minimize the PAPR at the CFR output, while respecting a pair of constraints related to acceptable levels of signal distortions: error vector magnitude (EVM) and adjacent channel power ratio (ACPR). EVM is a metric that measures, in time domain, the distortions inside the signal main channel and is represented as follows:

$$EVM = \frac{\sqrt{\sum_{n=1}^{N_T} |y[n]-w[n]|^2}}{\sqrt{\sum_{n=1}^{N_T} |w[n]|^2}} \cdot 100\% \qquad (4)$$

where $y[n]$ and $w[n]$ are the CFR output and input signals respectively and N_T is the total number of available samples. The distortions located outside the signal channel are quantified by the ACPR. Differently from EVM metric, this one works with signals in frequency domain and its value is given by:

$$ACPR = 10\log_{10}\left[\frac{\int_{adj} |Y(f)|^2 df}{\int_{main} |Y(f)|^2 df}\right] \qquad (5)$$

where the $Y(f)$ represents the frequency domain description of the CFR output signal and the indexes *adj* and *main* refer to adjacent and main channels, respectively.

Besides, to avoid instability problems, in case of IIR filter, a third constraint must be considered in order to guarantee that all the poles must not have amplitudes equal or larger than one.

In summary, the constrained optimization algorithm can be mathematically modeled as follows:

$$\min_x PAPR(x) \text{subject to} \begin{cases} EVM(x) \leq MAX_{EVM} \\ ACPR(x) \leq MAX_{ACPR} \\ \max\left[|Vector_{poles}(x)|\right] < 1 \end{cases} \qquad (6)$$

where $Vector_{poles}$ is a vector containing all the IIR filter poles, MAX_{EVM} a number that indicates the maximum tolerable level of EVM distortion, MAX_{ACPR} a number that indicates the maximum acceptable level of ACPR distortion and x indicates the vector of optimization variables, which includes L from (1), together with either h_k from (2) or a_0, a_k and b_m from (3).

It is worth mentioning that the objective function and all the constraint functions depend on the optimization variables in a nonlinear way. Therefore, a nonlinear tool must be employed to perform such constrained optimization. Nonlinear algorithms demand for an initial guess for each optimization variable and can be trapped into local minima according to the starting point. Given the broader range of phenomena covered by the IIR filter, the optimizer performance is expected to be more sensitive to the IIR filter initial guess, especially for its poles.

V. MATLAB SIMULATION RESULTS

In this section, the limiter described in (1) and the FIR and IIR filters described in (2) and (3) were applied to the PAPR reduction of a test signal. The test signal consists in a sequence of 2048 time domain samples of a WCDMA complex-valued envelope having a bandwidth of 3.84 MHz, sampled at 61.44 MHz and showing a PAPR value equal to 9.7 dB.

The constrained nonlinear optimization is performed in Matlab software using the interior point algorithm [12] and double precision floating point arithmetic. The clipping factor L was initiated by a value within a closed interval between 0.3 and 0.8. The truncation factors M from (2) and (3), as well as N from (3), were set equal to 11. The initial guesses for the FIR filter coefficients were randomly selected in an open interval from 0 to 1. Concerning the IIR filter, the initial guesses for its coefficients were copied from a Butterworth low-pass filter approximation. A Butterworth low-pass filter approximation is given by [7]:

$$\left|H(\omega)\right| = \frac{1}{\sqrt{1+\left(\frac{\omega}{\omega_0}\right)^{2n}}} \tag{7}$$

where n is the filter order and ω_0 the filter cutoff frequency. In here n was set to 11 and ω_0 to 12.06 Mrad/s.

In relation to the optimization nonlinear constraints, it was set a maximum value for the EVM of 17.5% and for the ACPR of -45 dB. For the ACPR calculation, an adjacent channel of bandwidth equal to 3.84 MHz, and whose center is 5 MHz from the main channel center, was considered.

Table I shows the PAPR reduction provided by the two implemented CFRs that differ between them just by their linear digital filters. According to Table I, between the digital filters implemented and optimized in this work, the IIR filter obtained a PAPR reduction there is 1.5 dB larger than the one offered by the FIR filter, where this number is equivalent to 15.5% of the initial PAPR value. Therefore, if the extra concerns that appear in IIR filter designs, namely instability issues and susceptibility to initial conditions, are properly handled during the parameter identification, then a very significant further reduction in PAPR is achieved, in comparison with FIR filters, thanks to the superior modeling capability of IIR filters attributed to the presence of negative feedback.

TABLE I. SIMULATION RESULTS

CFR Filter	PAPR reduction
FIR	2.3 dB
IIR	3.8 dB

Figures 2, 3 and 4 illustrate how the CFR technique, with the limiter and linear filter optimized, acts to reduce the PAPR of the complex-valued envelope signal. Figure 2 shows waveforms of the CFR input and output amplitudes, for the realizations with the FIR and IIR filters. Figure 3 shows the power spectral densities (PSDs) of the CFR input and output signals, again for the realizations with IIR and FIR filters. Figure 4 shows the CFR output amplitude in function of the CFR input amplitude, once more for the two types of filters studied in this work. From Fig. 2, it is noticed that the two implemented CFRs reduced the PAPR by clipping the input signal peaks. In a comparison between the two filters, Fig. 2 clearly illustrates that the CFR implemented with IIR filter provides a much more significant decline of the signal peaks.

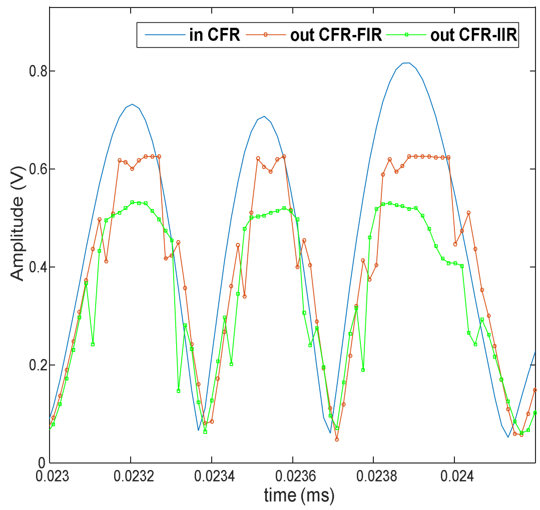

Fig. 2. Amplitude waveforms at CFR input and output.

From Fig. 3, it is observed that the CFRs inserted distortions at adjacent channels of the complex-valued envelopes. In particular, the CFR output with IIR filter presented larger distortions than the CFR output with FIR filter. Hence, the extra PAPR reduction offered by the IIR filter, in comparison with the FIR filter, can be related to its more aggressive use of the available distortion margin at adjacent channels, as illustrated in Fig. 3. The transfer characteristics shown in Fig. 4 evidence that the CFR not only manipulate in a nonlinear way the complex-valued envelope, asserted by the gain compression and saturation mechanisms, but also aggregate memory effects due to the scattering aspect of the curves. A comparison between the two approaches shows that the CFR output with FIR filter saturates at a higher amplitude level (around 0.6 V) with respect to the CFR output with IIR filter (around 0.5 V).

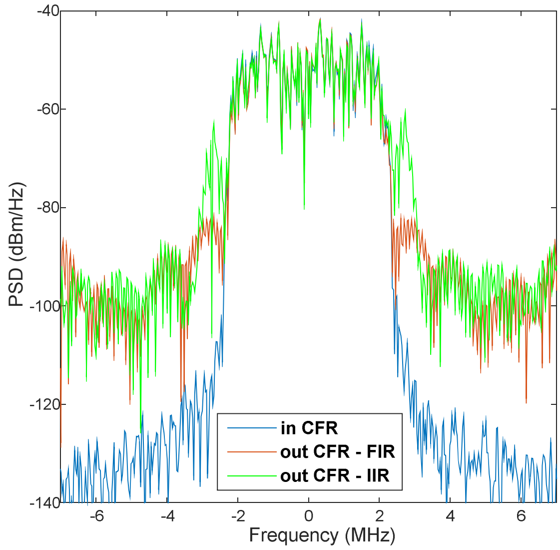

Fig. 3. Power spectral densities at CFR input and output.

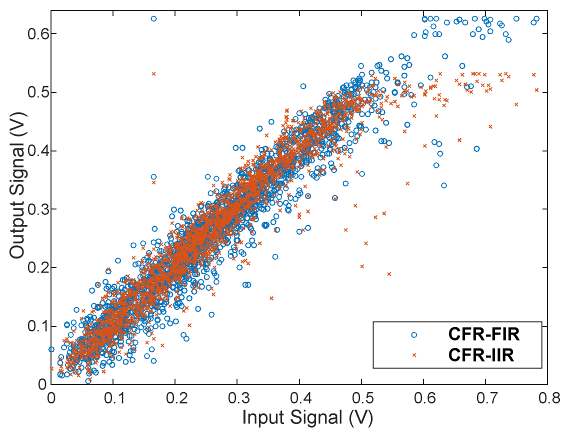

Fig. 4. CFR output amplitude in function of CFR input amplitude, for FIR and IIR filters.

VI. Conclusions

In this work, the CFR technique was approached, which is composed by a hard-clipping limiter and a linear digital filter. Both FIR and IIR filter realizations were implemented in this work. The instability issue in IIR filters was handled by adding a constraint in the nonlinear optimization procedure. While the FIR filter coefficients can be initiated by random values without compromising the quality of the identified parameters, the initial guess for IIR filters must be carefully chosen to avoid the training algorithm to be trapped into local minima. Based on simulation results from a WCDMA test signal and interior point algorithm, by using as initial values for the IIR filter the coefficients of a Butterworth low-pass approximation, a further 1.5 dB reduction in PAPR was achieved by means of the IIR filter instead of the FIR filter. A future direction for this work is to address the power consumption of a fixed-point arithmetic hardware implementation of the CFR technique in field programmable gate arrays or application specific integrated circuits.

Acknowledgment

The authors would like to acknowledge the financial support provided by Programa de Iniciação Científica da Universidade Federal do Paraná, modalidade UFPR/Tesouro Nacional, and by Pró-Reitoria de Assuntos Estudantis (PRAE-UFPR).

References

[1] D. Raychaudhuri and N. B. Mandayam, "Frontiers of Wireless and Mobile Communications," *Proceedings of the IEEE* , vol.100, no.4, pp.824-840, Apr. 2012.

[2] S. Cripps, *RF Power Amplifiers for Wireless Communications*, 2nd edition. Norwood, MA: Artech House, 2006.

[3] P. B. Kenington, *High Linearity RF Amplifier Design*. Norwood, MA: Artech House, 2000.

[4] C. Nader, P. N. Landin, W. V. Moer, N. Björsell, and P. Händel, "Performance Evaluation of Peak-to-Average Power Ratio Reduction and Digital Pre-Distortion for OFDM Based Systems," *IEEE Trans. Microw. Theory Tech.*, vol. 59, no. 12, pp. 3504–3511, Dec. 2011.

[5] X. Li and L. Cimini, "Effects of clipping and filtering on the performance of OFDM," *IEEE Commun. Lett.*, vol. 2, no. 5, pp. 131–133, May 1998.

[6] L. D. Silva and E. G. Lima, "Estudo Comparativo de Filtros Digitais FIR com Aplicação na Redução da Razão entre as Potências de Pico e Média em Sistemas de Comunicações sem Fio," in *XXII Iberchip Workshop*, Feb. 2016, pp. 9-12.

[7] A. V. Oppenheim, A. S. Willsky, and S. H. Nawab, *Signals & Systems,* 2nd edition. Upper Saddle River, NJ: Prentice Hall, 1997.

[8] B. Razavi, *Fundamentals of microelectronics*, 2nd edition. New York, NY: John Wiley & Sons, 2013.

[9] T. W. Parks and C. S. Burrus, *Digital Filter Design*. New York, NY: John Wiley & Sons, 1987.

[10] V. K. Ingle and J. G. Proakis, *Digital Signal Processing using Matlab®,* 3rd Edition. Cengage Learning, 2012.

[11] A. V. Oppenheim, R. W. Schafer, and J. R. Buck, *Discrete-time Signal Processing*. Upper Saddle River, NJ: Prentice Hall, 1998.

[12] R. A. Waltz, J. L. Morales, J. Nocedal, and D. Orban, "An interior algorithm for nonlinear optimization that combines line search and trust region steps", *Mathematical Programming*, vol. 107, no. 3, pp. 391–408, 2006.